Glycobiology vol. 19 no. 4 pp. 437–450, 2009
doi:10.1093/glycob/cwn158
Advance Access publication on January 7, 2009

Highly fucosylated *N*-glycan ligands for mannan-binding protein expressed specifically on CD26 (DPPVI) isolated from a human colorectal carcinoma cell line, SW1116

Nobuko Kawasaki[2], Chia-Wei Lin[3,4], Risa Inoue[2], Kay-Hooi Khoo[3,4], Nana Kawasaki[5], Bruce Yong Ma[2], Shogo Oka[6], Masaji Ishiguro[7], Toshihiko Sawada[8], Hideharu Ishida[8], Tomohiro Hashimoto[9], and Toshisuke Kawasaki[1,2]

[2]Research Center for Glycobiotechnology, Ritsumeikan University, Shiga 525-8577, Japan; [3]Institute of Biological Chemistry, Academia Sinica, Taipei 11529; [4]Graduate Institute of Biochemical Sciences, National Taiwan University, Taipei 106, Taiwan; [5]Division of Biological Chemistry and Biologicals, National Institute of Health Sciences, Tokyo 158-8501, Japan; [6]Human Health Sciences, Graduate School of Medicine, Kyoto University, Kyoto 606-8507, Japan; [7]Suntory Institute for Bioorganic Research, Osaka 618-8503, Japan; [8]Faculty of Applied Biological Sciences, Gifu University, Gifu 501-1193; and [9]Faculty of Regional Studies, Gifu University, Gifu 501-1193, Japan

Received on September 30, 2008; revised on December 24, 2008; accepted on December 27, 2008

The serum mannan-binding protein (MBP) is a host defense C-type lectin specific for mannose, *N*-acetylglucosamine, and fucose residues, and exhibits growth inhibitory activity toward human colorectal carcinoma cells. The MBP-ligand oligosaccharides (MLO) isolated from a human colorectal carcinoma cell line, SW1116, are large, multiantennary *N*-glycans with highly fucosylated polylactosamine-type structures having Le^b–Le^a or tandem repeats of the Le^a structure at their nonreducing ends. In this study, we isolated the major MBP-ligand glycoproteins from SW1116 cell lysates with an MBP column and identified them as CD26/dipeptidyl peptidase IV (DPPIV) (110 kDa) and CD98 heavy chain (CD98hc)/4F2hc (82 kDa). Glycosidase digestion revealed that CD26 contained such complex-type *N*-glycans that appear to mediate the MBP binding. MALDI-MS of the *N*-glycans released from CD26 by PNGase F demonstrated conclusively that CD26 is the major MLO-carrying protein. More interestingly, a comparison of the *N*-glycans released from the MBP-binding and non-MBP-binding glycopeptides suggested that complex-type *N*-glycans carrying a minimum of 4 Le^a/Le^b epitopes arranged either as multimeric tandem repeats or terminal epitopes on multiantennary structures are critically important for the high affinity binding to MBP. Analysis of the *N*-glycan attachment sites demonstrated that the high affinity MLO was expressed preferentially at some *N*-glycosylation sites, but this site preference was not so stringent. Finally, hypothetical 3D models of tandem repeats of the Le^a epitope and the MBP-Lewis oligosaccharide complex were presented.

[1]To whom correspondence should be addressed: Tel: +81-77-561-3444; Fax: +81-77-561-3496; e-mail: tkawasak@fc.ritsumei.ac.jp

Keywords: CD26/Le^a epitope/mannan-binding lectin/mannan-binding protein/SW1116

Introduction

The mannan-binding protein (MBP), also called mannose-binding protein (MBP) or mannan-binding lectin (MBL), is a C-type lectin specific for mannose, *N*-acetylglucosamine, and fucose residues (Kawasaki et al. 1983; Kawasaki 1999; Takahashi et al. 2005; Dommett et al. 2006; Taylor and Drickamer 2007). MBP is an important serum component associated with innate immunity (Kawasaki et al. 1989; Super et al. 1989; Hoffmann et al. 1999). MBP activates complement when it binds to oligosaccharide ligands on the surface of microorganisms (Ikeda et al. 1987). This pathway is called the lectin pathway (Malhotra et al. 1994). The most important property of this host defense system is the distinction between host cells and microorganisms based on the nature of their cell surface carbohydrates. MBP binds to mannooligosaccharide structures on the surfaces of microorganisms, whereas most mammalian cells are covered with complex oligosaccharides with sialic acids at their nonreducing termini, which precludes the binding of MBP to the cells. However, we and others previously noticed that MBP binds to some human tumor cell lines, suggesting the possibility that MBP also functions as a defense factor against abnormal cells produced in host animals (Ohta and Kawasaki 1994; Muto et al. 1999). In the following study, we found that the vaccinia virus carrying the human MBP gene exhibited potent growth inhibitory activity toward human colorectal carcinoma, SW1116, cells in nude mice via a complement-independent mechanism (Ma et al. 1999). We have proposed calling this activity MBP-dependent cell-mediated cytotoxicity (MDCC).

In our previous study, we isolated and characterized the endogenous MBP-ligand oligosaccharides (MLO) expressed on SW1116 cells, which were assumed to be associated with MDCC (Terada et al. 2005). The MLO on SW1116 cells were *N*-glycans with highly fucosylated polylactosamine-type structures and large molecular sizes. At their nonreducing termini, Le^b–Le^a or tandem repeats of the Le^a structure prevailed, a substantial proportion of which were attached via internal Le^x or *N*-acetyllactosamine units to the trimannosyl fucosylated core. This novel structure may represent a new type of tumor-associated carbohydrate antigen.

In this study, we attempted to identify and characterize the glycoproteins carrying the MLO with the unique structure. By using an MBP-affinity column, two major MBP-ligand glycoproteins (MLGPs) were isolated and identified as CD26 (dipeptidyl peptidase IV (DPPIV)) and CD98 heavy chain (CD98hc). The digestion of these MLGPs with PNGase F and endo-β-*N*-acetylglucosaminidase H (endo H) indicated that the

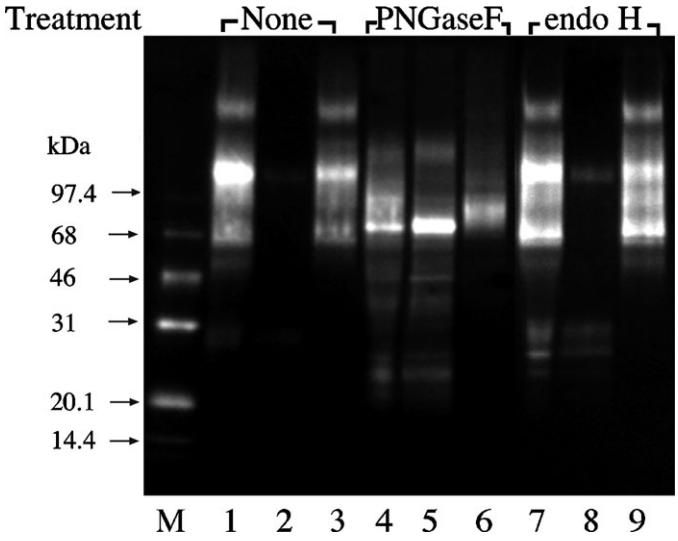

Fig. 1. Isolation of cell surface glycoproteins carrying MBP ligands from SW1116 cells and their susceptibility to glycosidase digestion. SW1116 cells were surface-labeled with sulfo-NHS-biotin and lysed in 1.0% Nonidet P-40-containing buffer, and then the lysates were applied to an MBP column. The eluate with the EDTA-containing buffer from the MBP column was then applied to an immobilized monomeric avidin column, as described under *Material and methods*. Then, the biotinylated MBP-ligand glycoproteins were analyzed for susceptibility to glycosidase digestion for 18 h at 37°C with PNGase F or endo H. After deglycosylation treatment, the control (no enzyme) and enzyme-treated proteins were applied to a second MBP-affinity column. Each sample before application to the second MBP column, and the pass-through and eluated fractions were resolved by SDS–PAGE on a 5–20% gradient gel under reducing conditions. The labeled proteins were transferred to a nitrocellulose membrane, and then detected with horseradish peroxidase-conjugated streptavidin. Lanes 1–3, samples without glycosidase digestion; lanes 4–6, samples after PNGase F digestion; lanes 7–9, samples after endo H digestion. Lanes 1, 4, and 7, an aliquot before application to the second MBP column; lanes 2, 5, and 8, pass-through fraction from the second MBP column; lanes 3, 6, and 9, eluated fraction from the second MBP column. Lane M, molecular weight markers.

characteristic MLO was attached to CD26. Chymotryptic digests of CD26 were fractionated into MBP-binding glycopeptides and non-MBP-binding glycopeptides. Subsequent structural analysis of these two glycopeptide fractions demonstrated that complex-type *N*-glycans with larger than four Fuc(Hex-HexNAc) units are critical for the high affinity binding to MBP.

Results

Characterization of cell surface MBP-ligand glycoproteins

The cell surface glycoprotein fraction that contained MBP ligands was isolated from SW1116 cells, which had been labeled using sulfo-NHS-biotin, by means of an MBP-affinity column followed by a monomeric avidin-affinity column. Upon SDS–PAGE under reducing conditions, the fraction was shown to contain one major protein band of 110 kDa and a couple of minor protein bands, which were detected after visualization by a chemiluminescence staining method using horseradish peroxidase-conjugated streptavidin (see Figure 1, lane 1). All these proteins were recovered in the eluated fraction of the second MBP column (lane 3), and no visible protein was recovered in the pass-through fraction (lane 2) as was expected. After PNGase F digestion, the molecular size of the major protein band was significantly reduced (lane 4), and most of the proteins were recovered in the pass-through fraction (lane 5), indicating that they lost the binding activity to an MBP column almost completely. In contrast, after endo H digestion, no significant change was generated in their protein profiles (lane 1 versus lane 7), and all proteins retained their MBP-binding activity as evidenced by the absence of protein bands in lane 8 and the close resemblance of the protein profiles between lane 7 and lane 9. These experiments demonstrated clearly that the cell surface MLGPs consisted mainly of complex-type *N*-glycans and not of high-mannose-type or hybrid-type *N*-glycans. However, it may be worthy of note that a broad protein band of around 80 kDa was detected in lane 6 (the eluated fraction of the second MBP column), inferring the presence of PNGase F-resistant MBP-binding components such as mucin-type glycoproteins. In fact, our preliminary experiments indicated that the MBP-binding activity of the SW1116 cells analyzed by flow cytometry using FITC-labeled MBP was reduced significantly by the pretreatment of the cells with benzyl-2-acetamide-2-deoxy-α-galactopyranoside (Bz−α-GalNAc), an inhibitor of *O*-glycan biosynthesis (Huang et al. 1992) (data not shown).

Isolation and identification of MBP-ligand glycoproteins from SW1116 cell lysates

In order to identify the carrier proteins of the MLO having the unique structure, SW1116 cell lysates were applied to an AAL (*Aleuria aurantia* lectin)-agarose column, which binds the Fucα1-6 structure most preferentially followed by the Fucα1-2 and Fucα1-3 structures (Yamashita et al. 1985), and subsequently to an anti-Le^b mAb-Sepharose 4B column and an MBP-Sepharose 4B column. The proteins bound to the MBP column in the presence of calcium were eluted with EDTA, and then resolved by SDS–PAGE under reducing conditions. As shown in Figure 2A, two major protein bands were observed. LC-MS/MS analysis of the *in-gel* trypsin digests of these two bands indicated that the 110 kDa protein was CD26/dipeptidyl peptidase IV (DPPIV) and the 82 kDa protein was CD98 heavy chain (CD98hc)/4F2hc. The amino acid sequences corresponding to those of the respective proteins are shown in red in Figure 2B. CD26 and CD98hc are proteins that have nine and four potential *N*-glycosylation sites, respectively, as shown by yellow-shaded areas in their primary sequences.

MBP-binding activity of MBP-ligand glycoproteins after glycosidase digestion

The properties of the oligosaccharides attached to these glycoproteins were examined by means of glycosidase digestion and MBP lectin blot. Upon PNGase F digestion, the CD26 protein band (110 kDa) disappeared almost completely and a new band appeared at around 85 kDa, while the molecular size of CD98hc did not change significantly (data not shown). On the other hand, the MBP-binding activities of both CD26 and CD98hc, as examined by MBP blotting, were completely lost upon PNGase F digestion, as shown in Figure 3A, lane 1 (as compared to lane 2, which is without PNGase F digestion). In contrast, upon endo H digestion, CD98hc lost the MBP-binding activity almost completely, whereas CD26 retained a significant portion of the MBP-binding activity (lane 3). These results indicated that CD98hc contains high-mannose-type or

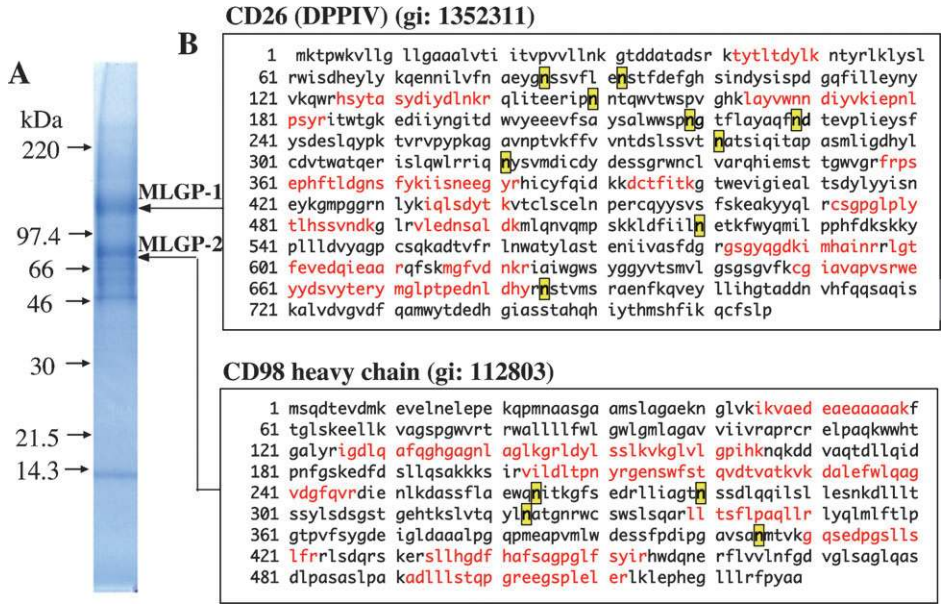

Fig. 2. Isolation and identification of the glycoproteins carrying MBP ligands from SW1116 cell lysates. MBP-ligand glycoproteins were purified from SW1116 cell lysates with AAL-, anti-Le^b mAb-, and MBP-affinity columns, and resolved by SDS–PAGE on a 5–20% gradient gel under reducing conditions, as described under *Material and methods*. (**A**) Colloidal Coomassie brilliant blue staining of the gel. The arrows (MLGP-1 and MLGP-2) indicate the major MBP-ligand glycoproteins. The positions of molecular weight markers are shown in the left margin. The bands MLGP-1 and MLGP-2 were excised and digested with trypsin, and the fragments from each band were used for the identification of MBP-ligand proteins by mass spectrometry, as described under *Material and methods*. (**B**) The results of a search against the human protein database of the National Center for Biotechnology Information based on the acquired fragmentation spectra of peptides. The identified peptides are shown in red within the complete CD26 and CD98hc sequences. The potential *N*-glycosylation sites are shown by yellow-shaded areas.

hybrid-type oligosaccharides, which are responsible for the MBP binding by CD98hc, whereas CD26 appears to contain the target oligosaccharides of the present study, highly fucosylated polylactosamine-type glycans of MBP ligands (MLO) as well as high-mannose-type or hybrid-type oligosaccharides. We also examined the protein profiles of CD26 and CD98hc before and after endo H digestion in order to obtain structural information accompanied with the reduction of the MBP-binding activity. However, the observed shifts in the respective molecular sizes of CD26 and CD98hc after endo H digestion were not so significant (data not shown) that it is difficult to explore this problem further at present.

MALDI-MS mapping of the permethylated N-glycans released in-gel from CD26

To ascertain if CD26 carries the unique MBP ligands (MLO) comprising multimeric Le^a/Le^b, its *N*-glycans were released *in-gel* with PNGase F for MS analyses from the single protein band (Figure 3B) corresponding to CD26 isolated consecutively with AAL-, MBP-, and anti-human CD26 mAb affinity columns from SW1116 cell lysates. As shown in Figure 4A, the major molecular ion signals observed on MALDI-MS analysis of the permethylated *N*-glycans correspond to $[M+Na]^+$ of a hybrid-type *N*-glycans with 1 Fuc(Hex-HexNAc) terminal, followed by complex-type *N*-glycans with 2 Fuc(Hex-HexNAc) termini, and go up by multiples (up to 6) of Fuc(Hex-HexNAc) increments, as annotated. Composition-wise, the majority of the signals appear to also reflect core fucosylation and a bisecting GlcNAc, while a small amount was further sialylated. Additional high-mannose-type *N*-glycans (Man5-Man7) were also detected. More importantly, the overall profile is fully consistent with a subset of the CD26 *N*-glycans carrying the requisite MLO as isolated and defined previously from SW1116 cell lysates (Terada et al. 2005), the removal of which by PNGase F would lead to the loss of MBP binding (Figure 3A, lane 1). Given the size and structural heterogeneity, it could also be predicted that the smaller bi- and triantennary *N*-glycans would not constitute high affinity MLO despite the similar presence of Fuc(Hex-HexNAc) terminal epitopes, and that not all *N*-glycosylation sites may contribute equally to MBP binding. To substantiate this, it would be of interest to determine which glycopeptides would be recovered in the MBP-binding and non-MBP-binding fractions, respectively.

Analysis of MBP-binding and non-MBP-binding glycopeptides from chymotryptic digests of CD26

The extreme heterogeneity and large size of the MLO imposed a significant technical challenge as to the detection and identification directly of the intact glycopeptides by MS analyses. In a pilot experiment, it was found that the chymotrypsin-digested products derived from the ^{3}H-glucosamine-labeled CD26 afforded a better recovery (88%) of the radioactivity on an MBP column, where the radioactivities distributed in the pass-through and binding fractions were 72% and 28%, respectively. For subsequent studies, the MBP-binding and non-MBP-binding glycopeptides were therefore prepared from chymotrypsin digests of the cold CD26 sample, instead of the more commonly used trypsin. After desalting, the *N*-glycans and de-*N*-glycosylated peptides were analyzed by MS separately. At first glance, the *N*-glycan profile of the non-MBP-binding fraction (Figure 4B) resembles that of the total *N*-glycans derived from *in-gel* digested CD26 (Figure 4A), whereas no significant *N*-glycan

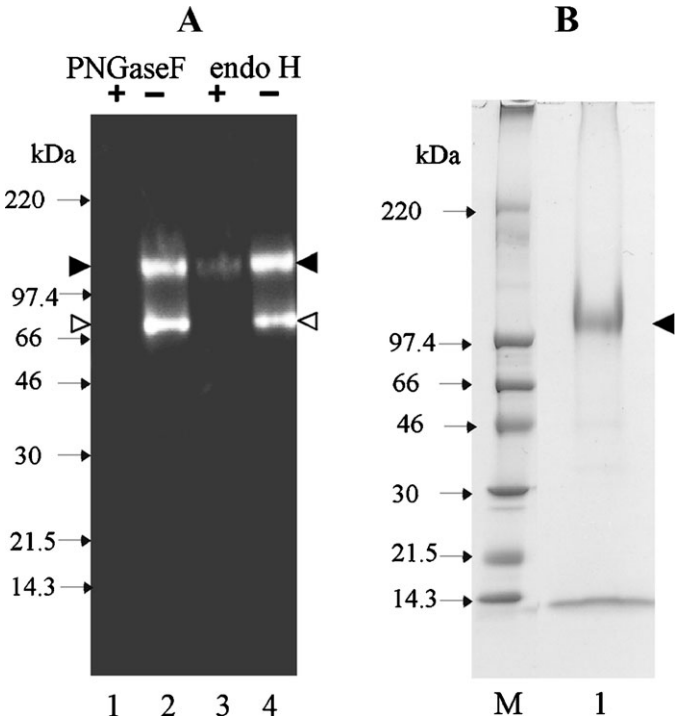

Fig. 3. Effects of glycosidase digestion on MBP-binding activity of the MBP-ligand glycoproteins (A) and purification of CD26 from MBP-ligand glycoproteins on an anti-human CD26 mAb column (B). (**A**) The MBP-ligand glycoproteins, purified from SW1116 cell lysates with AAL-, anti-Le^b mAb-, and MBP-affinity columns, were analyzed for susceptibility to glycosidase digestion by treatment with PNGase F or endo H at 37°C for 18 h. After deglycosylation treatment, the control and treated proteins were resolved by SDS–PAGE on a 5–20% gradient gel under reducing conditions, and then the proteins were transferred to a nitrocellulose membrane, followed by MBP lectin-blot detection as described under *Material and methods*. MBP blotting after treatment of the MBP-ligand glycoproteins in the presence (+) and absence (−) of PNGase F (lanes 1 and 2) or endo H (lanes 3 and 4). The filled arrowhead indicated the position of the CD26 band and open arrowhead CD98hc. The positions of molecular weight markers are shown in the left margin. (**B**) CD 26 was isolated using an anti-human CD26 mAb-Sepharose 4B column from the MBP-ligand glycoproteins, which had been isolated with AAL and MBP-affinity columns, and resolved by SDS–PAGE on a 5–20% gradient gel under reducing conditions. The proteins were detected by colloidal Coomassie brilliant blue staining. The arrowhead indicates the purified CD26 band (lane 1). Lane M, molecular weight markers.

signal was detected for the sample derived from the MBP-binding fraction (data not shown), when analyzed by MALDI-MS in the reflectron mode. However, closer examination revealed that the signal intensities of larger complex-type *N*-glycans, particularly for those above *m/z* 3800, corresponding to having more than four Fuc(Hex-HexNAc) units, appeared to be significantly lower relative to the one with two Fuc(Hex-HexNAc) termini (*m/z* 2837), in the nonbinding fraction. With linear mode MALDI-MS, which is more conducive for detecting species of higher molecular mass, albeit with lower resolution, it is clear that the *N*-glycan profiles derived from the non-MBP-binding fraction afforded a major signal at *m/z* 3460, corresponding to having three Fuc(Hex-HexNAc) units, and extended mostly to just above *m/z* 5000, components carrying a total of four to six Fuc(Hex-HexNAc) units affording only very weak signals (Figure 5A). In contrast, the MBP-binding fraction, which did not give any significant *N*-glycan signals in the reflectron mode, afforded major signals above *m/z* 3900, corresponding to having four Fuc(Hex-HexNAc) units, and extending up to about *m/z* 6400, corresponding to having five to seven Fuc(Hex-HexNAc) units (Figure 5B). This striking pattern demonstrated clearly that glycopeptides from CD26 that could bind efficiently to an MBP column carried mostly complex-type *N*-glycans with at least four Fuc(Hex-HexNAc) units. As a consequence of these larger glycopeptides being preferentially enriched in the binding fraction, the nonbinding fraction in turn contained less of these relative to those smaller ones. Conversely, the glycopeptides with bi- and tri-antennary complex-type *N*-glycans were found mostly in the nonbinding fraction. It should be further noted that glycopeptides carrying high-mannose structures were also clearly not MLO as these glycans were likewise prominently detected only in the nonbinding fraction.

To identify the respective glycosylation sites represented by the glycopeptides in the binding and nonbinding fractions, the de-*N*-glycosylated peptides were subjected to automated nanoLC-ESI-MS/MS analyses, and the resulting MS/MS data were matched against the CD26 protein sequence by means of Mascot search, as well as by further manual interpretation of the de novo sequencing data. Through the latter process, it was found that peptide matching or coverage was substantially improved by not specifying chymotrypsin in the database search. This was due to an unexpectedly high degree of nonspecific cleavage induced by chymotrypsin and the lengthy isolation procedure employed. Furthermore, it was found that most peptides were additionally modified at their N-termini through carbamylation, most likely due to the use of urea in the digestion, which produced isocyanic acid that would react with primary amine groups. Taking these factors into consideration for the search criteria and manual data interpretation, peptides encompassing seven out of nine potential *N*-glycosylation sites were identified in the nonbinding fractions (Figure 6). The PNGase F-treated peptides carrying these NXS/T sites all exhibited conversion of Asn to Asp, with a mass increment of one unit, thus suggesting that all these seven sites (N85, 92, 150, 229, 281, 520, and 685) were originally *N*-glycosylated since the Asn residue at a nonoccupied site would remain as such. The two other sites at N219 and N321 were not identified, which was most likely due to their being too small in size to be detected via LC-MS/MS or they might have been lost in the first place on the Sephadex G-10 column used for desalting. Similar LC-MS/MS analysis of the binding fraction followed by an MS/MS ion search using the same criteria as described above (carbamylation, nonspecific cleavage, and Asn to Asp conversion) led to unambiguous identification of five *N*-glycosylated sites (N85, 92, 150, 229, and 685). The two sites at N281 and N520, which could be identified in the nonbinding fraction, were not detected in the binding fraction, whereas the two sites at N219 and N321 were not detected in either fraction. Since the chymotryptic peptide carrying N520 gave a good MS response and good quality MS/MS data for the non-MBP-binding fraction, it may be inferred that it indeed did not carry high affinity MBP ligands and therefore could not be found in the MBP-binding fraction, which would otherwise be readily detected. Overall, it may be concluded that most glycosylation sites (at least five out of the seven identified) are equally heterogeneous in their *N*-glycosylation profile, comprising both MBP ligands and non-ligand glycoforms at variable proportions. The site at N520, for example, may carry mostly smaller, non-MBP-binding

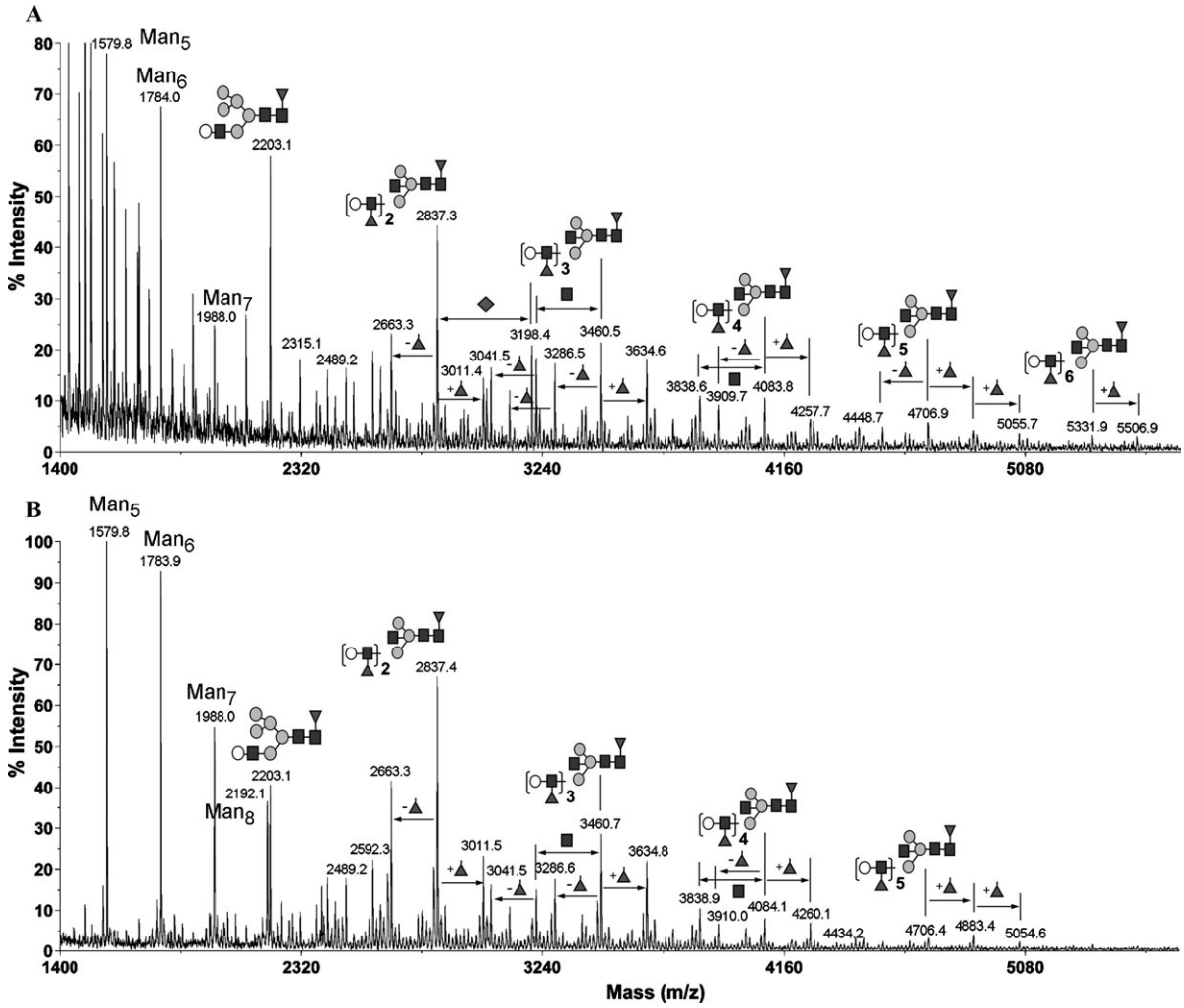

Fig. 4. MALDI-MS mapping of the permethylated *N*-glycans released *in-gel* from the CD26 protein band (**A**) and from non-MBP-binding chymotryptic peptides of CD26 (**B**), in the reflectron mode. The *N*-glycan profile of the nonbinding glycopeptide fraction resembles the total *N*-glycan profile of the CD26 but is notably cleaner with more prominent signals corresponding to high-mannose-type structures. When also analyzed in the reflectron mode, the bound glycopeptide fraction did not afford any meaningful *N*-glycan signals (data not shown). The major sodiated molecular ion series could be assigned as core fucosylated, bisected complex-type *N*-glycans with 2-6 Fuc(Hex-HexNAc) units based on the molecular composition and previously characterized structures for MBP ligands (Terada et al. 2005), as annotated. Each is accompanied by an additional degree of fucosylation (▲). Heterogeneity also arises from the lack of the extra bisecting GlcNAc (■) and/or additional sialylation (♦). (○,●) Represents Hex (Gal, Man). For simplicity and to avoid overcrowded annotation, not all signals are annotated.

N-glycans because the majority of these were not retained by the MBP column.

The three-dimensional structure of the extracellular domain (39-766) of human CD26 (type II transmembrane, glycosylated), which was produced using a recombinant baculovirus system, is shown in Figure 7, being cited from K Aertgeerts et al. (2004) with modification. Seven (N229, N150, N281, N219, N92, N85, and N321) of the nine potential *N*-glycosylation sites were in the propeller domain of the molecule (blue), and two sites (N685 and N520) were in the hydrolase domain (red). Seven sites (N685 and N520 in the hydrolase domain and N229, N150, N281, N92, and N85 in the propeller domain) were found to be glycosylated but two sites, N321 and N219 (indicated by gray circles), were not identified. It should be noted that N281 and N520 (green circles) were found in the nonbinding fraction but not in the binding fraction, and the other sites that were marked doubly by green and pink circles were found not only in the binding fraction but also in the nonbinding fraction.

Model structure of the MBP-Lewis oligosaccharides complex

The observations that the MBP column binding glycopeptides carried mostly complex-type *N*-glycans with at least four Fuc(Hex-HexNAc) units while the nonbinding fraction in turn contained *N*-glycans with two or three Fuc(Hex-HexNAc) units and the ones with high-mannose structures suggested the possibility that four Fuc(Hex-HexNAc) units may have a certain unique conformation preferable for the high affinity binding to MBP. In accordance with this hypothesis, computer modeling suggested the possibility that the tandem repeat structure of the Le^a unit can form a right-handed helix in which equivalent positions recur every eight Le^a units, as shown in Figure 8A. In addition, viewing the Le^a α helix from the top, we find that fucose residues extend away from the long axis of the chain and every fourth fucose residue recurs at an equivalent position (Figure 8B). This unique topology of fucose residues in the Le^a α helix may be relevant to the high affinity binding of these ligands to MBP.

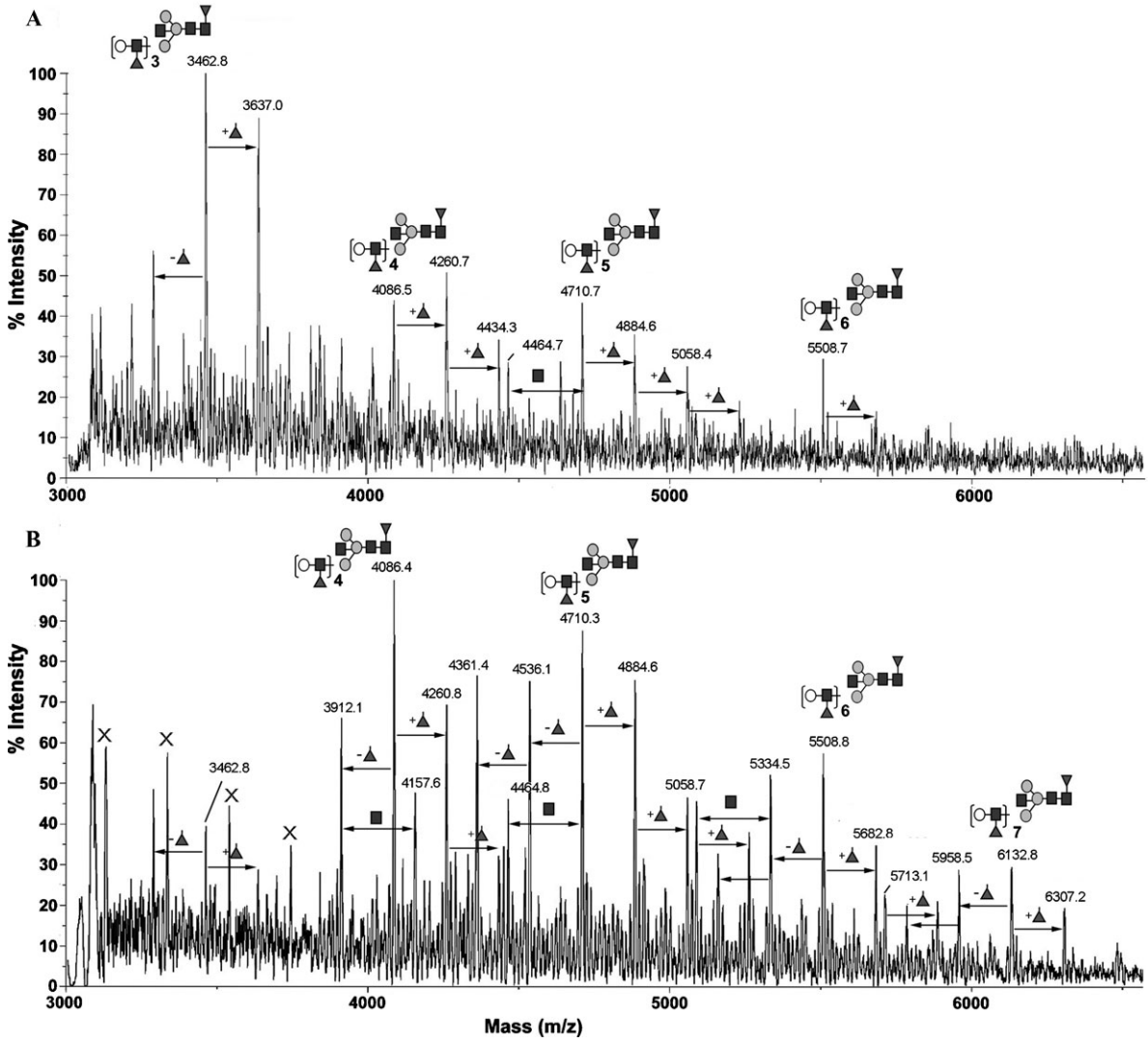

Fig. 5. MALDI-MS mapping of the permethylated *N*-glycans released from non-MBP-binding (**A**) and binding (**B**) chymotryptic peptides of CD26, in the linear mode. The *m/z* values of the annotated peaks refer to the average masses due to the poor resolution in the linear mode, which are normally 3–4 Da higher than the corresponding accurate monoisotopic signals in this mass range (used for the reflectron mode spectra in Figure 4). The symbols used are the same as in Figure 4. Peaks denoted by X are polyhexose contaminants.

Figure 9A shows a model structure of the MBP-Lewis oligosaccharides complex between the trimeric structure of carbohydrate recognition domain (CRD) and Le^b-$(Le^a)_4$-Le^x, a typical example of the nonreducing terminal oligosaccharide structure of MLO (see Figure 12 in Terada et al. 2005). Of the two fucose residues in the Le^b unit, the one in the Le^a unit appears to contribute to the protein binding, and the other fucose residue on the penultimate Le^a unit feasibly interacts with Lys183 and Asp184 on the MBP molecule (Figure 9B). The binding of each oligosaccharide chain at the trimeric protein structure resulted in the formation of a bundle of three oligosaccharide chains with fucose–fucose and galactose–galactose interactions in the three Le^a units at the Le^x end. Since the bundle formation occurred at the Le^a unit at the Le^x end, the five tandem structures of the Le^a units (or four Le^a and one Le^b units) appear to be important for the bundle formation. A short model with the reduction of the number of the Le^a moieties did not allow the formation of the trimeric oligosaccharide bundle.

Discussion

In this study, a human colon cancer glycoprotein, which carries the endogenous ligands for serum lectin MBP, was identified as CD26 (DPPIV). We previously elucidated the characteristic structures of the endogenous oligosaccharide ligands for MBP on SW1116 cells. The MBP-oligosaccharides have the Le^b/Le^a structure or tandem repeats of the Le^a structure at their nonreducing termini (Terada et al. 2005). The cell surface labeling experiment indicated that the major MBP-binding glycoprotein on the surface of SW1116 cells was a 110 kDa protein, which was later identified as CD26. MALDI-MS analysis of the *N*-glycans released from the purified CD26 clearly showed the presence of unique MLO on the CD26 molecule. Initially, we assumed that all the *N*-glycans on the CD26 molecule bound to an MBP column, but this was not really the case. These results, however, provided us an opportunity to study the mode of carbohydrate recognition of MBP by comparing the structures of

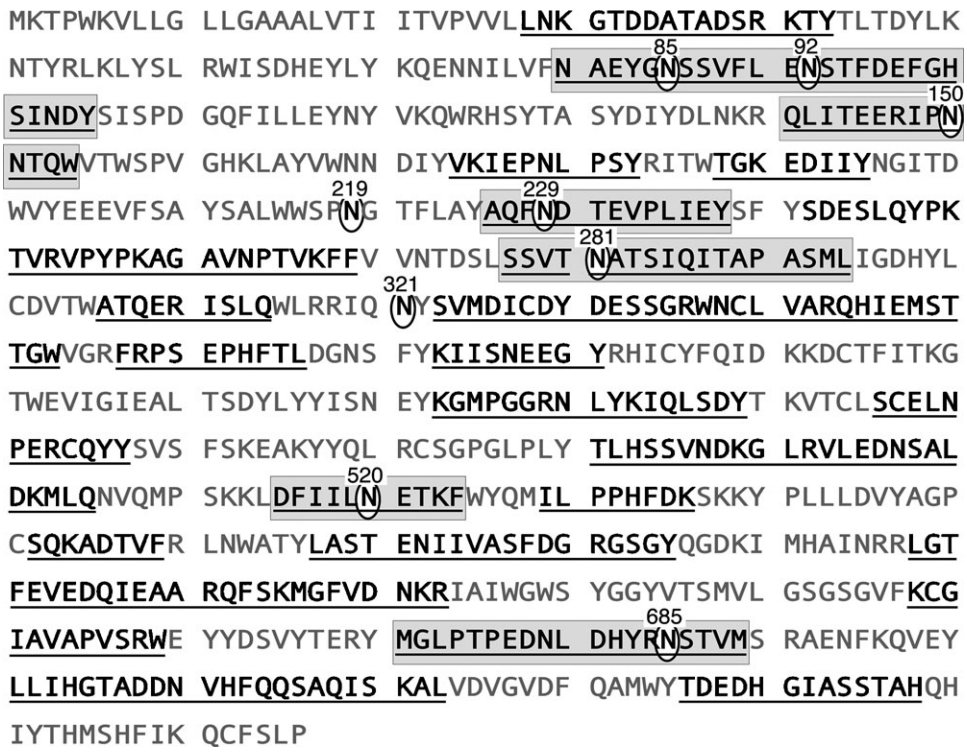

Fig. 6. The primary sequence of CD26 showing the protein coverage and the *N*-glycosylated sites identified on LC-MS/MS analysis of the de-*N*-glycosylated chymotryptic peptides derived from the non-MBP-binding fraction. The peptides identified, based on a search of the MS/MS data against the CD26 sequence with the settings described under *Material and methods*, are in black color and underlined. Nonidentified stretches are in gray. The Asn at potential *N*-glycosylation sites are circled and the amino acid residue numbers are labeled. The identified de-*N*-glycosylated peptides with Asn converted to Asp are boxed. All but N281 and N520 were also identified on similar analysis of the glycopeptides from the MBP-binding fraction. Peptides carrying the two potential *N*-glycosylation sites N219 and N321 were not detected.

the MBP-binding glycans with those of non-MBP-binding glycans isolated from the same molecule, CD26. Intriguingly, the *N*-glycans released from the non-MBP-binding glycopeptides contained M5–M9 high-mannose-type glycans and complex-type glycans mostly smaller than those with three LacNAc units (the term "LacNAc" usually implies type 2, Galβ1-4GlcNAc, whereas in this paper it implies both type 1 and 2 units). In contrast, the *N*-glycans from MBP-binding glycopeptides contained complex-type glycans with more than four LacNAc units. These results are completely consistent with our previous finding that MLO comprises 5 to 13 LacNAc units (see Figure 3 in Terada et al. 2005). It was also shown in our previous report that the binding affinity of carbohydrate ligands to MBP depends markedly on the clustering or topological pattern of the ligand sugars. Such sequence may be those in which every one of the four Le^a/Le^b units binds to trimannosyl core to make tetraantennary *N*-glycans and/or Le^a/Le^b units present as tandem repeat on either antenna of *N*-glycans. With this regard, it is worthy of note that most of the MBP-binding activity of MLO was lost after endo-β-galactosidase digestion, where the distribution of the sizes of the digests was significantly smaller than those of the original MLO, although most of the digested oligosaccharides still bound to an AAL (fucose-binding) column (see Figure 6 in Terada et al. 2005). Interestingly, 3D-structure modeling indicated the unique topology of fucose residues in the Le^a α helix, which may be relevant to the high affinity binding of these ligands to MBP. In addition, the binding of each MLO chain at the trimeric protein structure of CRD of MBP resulted in the formation of a bundle of three oligosaccharide chains. These results are consistent with the view that host defense molecules associated with innate immunity like MBP recognize specific topological patterns generated by the ligand molecules. However, it is clear that elucidation of the precise mechanisms of MBP recognition requires further studies by NMR or X-ray crystallography using synthetic ligands, and the study along these lines is now in progress. With respect to the MBP recognition of the oligo-LacNAc units, we also studied the interaction between MBP and glycolipids with Le^a trisaccharide units (1–3) on the lactosylceramides, which were isolated and characterized from COLO205 cells very recently (Fan et al. 2008). The activity toward Le^a-LacCer (lactosylceramide), Le^a–Le^a–LacCer, and Le^a–Le^a–Le^a–LacCer was compared by means of surface plasmon resonance. The KD (M) value for MBP, calculated from kd/ka, of Le^a–Le^a–Le^a–LacCer was decreased by approx. 40-fold compared to those of Le^a–LacCer and Le^a–Le^a–LacCer (around $1–2 \times 10^{-7}$ M), indicating that the tandem structure of the Le^a epitope is important for high affinity binding of glycolipid ligands as well as oligosaccharide ligands (unpublished data).

CD26 is a 110 kDa cell surface glycoprotein expressed on various tissues, including epithelial cells of liver, intestine, and kidney and is involved in tumor development of certain human cancers (Iwata and Morimoto 1999; Pro and Dang 2004; Havre et al. 2008). Inamoto et al. (2007) recently reported that CD26 is highly expressed on the cell surface of malignant mesotheliomas and that a newly developed humanized anti-CD26 monoclonal

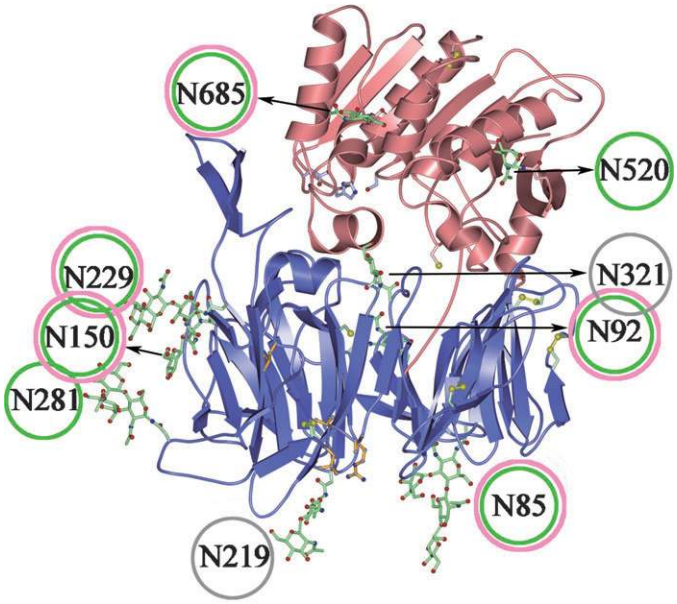

Fig. 7. The distribution of potential *N*-glycosylation sites between MBP-binding and non-MBP-binding glycopeptides of the CD26 molecule. The three-dimensional structure of the extracellular domain (39–766) of human CD26 is cited with slight modifications from Aertgeerts et al. (2004). The sugar molecules that were modeled into the electron density maps are shown in green as ball-and-stick representations. Seven of the nine glycosylation sites were found in the β-propeller domain of the molecule (blue), and two glycosylation sites were observed in the α/β-hydrolase domain (red) of the molecule. The green circles indicate the attachment sites of the glycans ($(Man)_5 \sim (Man)_8$, $\leq Le^a \times 3$) found in the CD26 non-MBP-binding glycopeptides. The pink circles indicate the attachment sites of the glycans ($\geq Le^a \times 4$) found in the CD26 MBP-binding glycopeptides. The gray circles show the potential *N*-glycosylation sites not identified in this study.

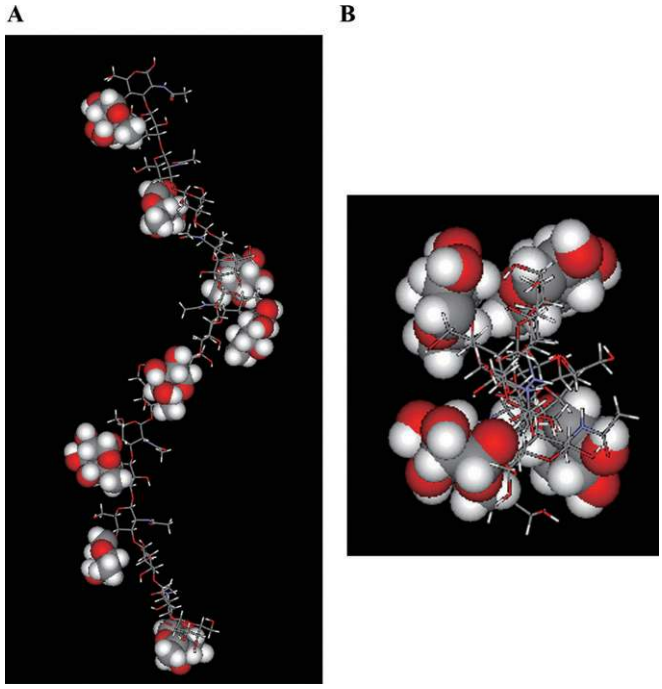

Fig. 8. 3D model of tandem repeats of the Le^a unit. (**A**) The side view of a right-handed helix of eight tandem repeats of the Le^a unit. The tandem repeat structure of the Le^a unit can form the right-handed helix in which equivalent positions in the helix recur every eight tandem repeats. The structure is depicted as a ball-and-stick model except for L-fucose, which is shown with a CPK model. (**B**) The view from the top of the four tandem repeats of the Le^a unit. L-Fucose residues are extended away from the long axis of the chain and every fourth fucose residue recur at the equivalent positions. Left lower fucose faces the front and the right lower fucose is located in the most remote place. The 3D modeling was performed as described under *Material and methods*.

antibody has an inhibitory effect on malignant mesothelioma cells both in vivo and in vitro via antibody-dependent cell-mediated cytotoxicity in addition to its direct anti-tumor effect. They also described that the anti-CD26 monoclonal antibody inhibits the growth of human renal carcinoma cells both in vitro and in vivo. Meanwhile, they found that the murine anti-CD26 mAb 14D10, from which the humanized anti-CD26 monoclonal antibody was constructed, recognized the cell membrane-proximal glycosylated region and has a direct anti-tumor effect by inducing G1-S arrest while concomitantly blocking the adhesion of cancer cells to the ECM. With this regard, it may be worthy of note that CD26 mAb 44-4, which was used for the purification of CD26 from SW1116 cell lysates in this study, lost its binding activity to the PNGase F-treated CD26 (data not shown), suggesting that the mAb 44-4 recognized the antigenic determinant containing *N*-glycans and/or the conformational structure in the vicinity of the *N*-glycan attachment sites. It may be reasonable to assume that the *N*-glycans with the unique structures of the Le^a epitope tandem repeats expressed on the CD26 molecules may be a molecular target for MBP and play a key role in triggering growth inhibitory activity toward a certain type of colon cancer cells that we call MDCC. Consequently, MBP may have potential clinical use as a novel cancer diagnostic and therapeutic agent for CD26-positive tumors, such as malignant mesotheliomas, CD26-positive T-cell malignancies (Ohnuma et al. 2002), and renal cell carcinomas (Inamoto et al. 2006), and various MBP-positive human colorectal cancer cells (Ohta and Kawasaki 1994; Muto et al. 1999) and tissues (unpublished data).

CD26 is known to be a highly glycosylated protein. However, the detailed structures of the *N*-glycans on the CD26 molecule have been little elucidated. In this study, using MS analyses, the structures of the *N*-glycans expressed on the CD26 molecule on the surface of human colon cancer cells, SW1116, and the *N*-glycosylation sites were characterized with respect to the ligands for a lectin, MBP. We have analyzed the distribution of the glycosylation sites between the non-MBP-binding and MBP-binding glycopeptides by means of the glycoproteomic-type approach. We could assign seven out of the total nine possible *N*-glycosylation sites in CD26. Two sites, N281 and N520, were found only in the MBP-non-binding glycopeptides, i.e., not in the MBP-binding fraction. Thus, these two sites probably do not carry MBP ligands. We may say that N281 and N520 were preferentially modified to Man5-7, simple hybrid-type or biantennary complex-type. Enzyme systems that synthesize MBP ligands (e.g., β3-galactosyltransferase (Fan et al. 2008)) disfavor N281 and N520 for some reason. However, five of the seven *N*-glycosylation sites identified, N85, N95, N150, N229, and N685, were recovered both in the MBP-non-binding and MBP-binding fractions. These results indicated that the unique MBP ligands were expressed preferentially at some

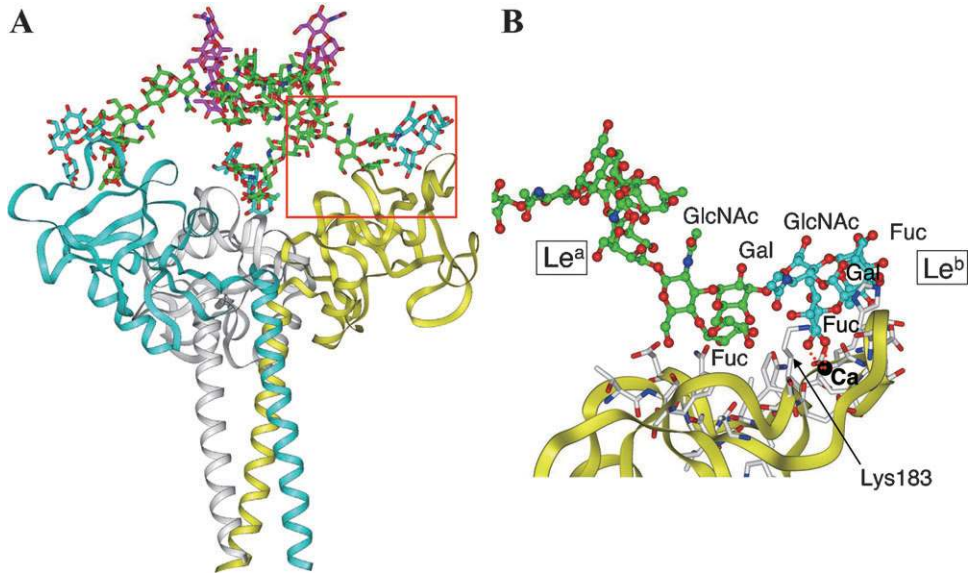

Fig. 9. 3D model of the MBP-Lewis oligosaccharides complex. (**A**) 3D model of the trimeric MBP-Lewis oligosaccharides complex. Oligosaccharide structures were constructed by use of the carbohydrate module installed in Insight II (Molecular Simulations Inc., San Diego, CA), and the structures were energy-minimized with molecular dynamics calculation in Discover3. The crystal structure of the trimeric mannan (mannose)-binding protein (pdb code: 1 kww) was used for building the complex model with the oligosaccharide fragment. The ribbon model of an MBP-trimer is represented by yellow, blue, and white ribbons, and the Lewis oligosaccharides are represented by ball-and-stick models. Le^b: light blue balls and sticks, Le^a: green balls and sticks, Le^x: magenta balls and sticks. (**B**) A close-up view of the area corresponding to the red line enclosed area in **A**. White sticks represent amino acids. A Ca ion interacts with L-Fuc in Le^b (light blue). L-Fuc in Le^a (green) adjacent to the terminal Le^b may also interact at the second site with Lys183 (black arrow) and Asp184 (not shown).

potential *N*-glycosylation sites but this site preference was not so stringent.

From the crystal structure of the extracellular domain (39-766) of human CD26 (type II transmembrane, glycosylated) produced using a recombinant baculovirus system (Figure 7), it has been inferred that all nine potential *N*-glycosylation sites are occupied based on the calculated electron-density maps (Aertgeerts et al. 2004). We do not know whether the two remaining potential *N*-glycosylation sites of the nine sites, namely N219 and N321, were glycosylated or not since these two peptides were not detected in either the MBP-binding or non-MBP-binding fraction. A possible cause is that the corresponding chymotryptic peptides may have been too short, especially if they are not glycosylated and/or with the extra nonspecific cleavages generally observed, for them to be efficiently recovered and detected. We prepared the chymotrypsin digested glycopeptides and peptides for MS analysis in this study based on the results of a pilot experiment involving a CD26 sample metabolically labeled with ^{3}H-glucosamine. In contrast with chymotrypsin digestion, the yields of trypsin digestion obtained from the starting amount through the steps before application to an MBP column were found not to be good and about half the peptides (and glycopeptides) seemed to become insoluble on trypsin digestion for some reason, and the recovery of the radioactivity on an MBP column was quite low (40%). Thus, glycopeptide preparation through CD26 tryptic digest was very difficult and unsuitable for the CD26.

The proteomic analysis of the MBP-binding glycoprotein fraction isolated from the SW1116 cell lysates suggested that the CD98 heavy chain (CD98hc), which had four potential *N*-glycosylation sites, might also carry MLO. However, the MBP-binding activity of CD98hc was abolished almost completely by endo H digestion, excluding the possibility that highly fucosylated polylactosamine-type structures are expressed on CD98hc and suggesting that high-mannose-type or hybrid-type oligosaccharides are associated with the MBP-binding activity. Since all glycoproteins carrying high-mannose-type oligosaccharides are not always good ligands for MBP, it is possible that CD98hc high-mannose-type oligosaccharides bind to MBP just by forming some specific three-dimensional complexes along the CD98 polypeptide backbone. This might also be the case in high-mannose-type glycans in CD26. In any case, CD98hc has also been reported to be related with tumorigenicity (Hara et al. 2000; Esseghir et al. 2006; Asano et al. 2007).

In summary, the present study demonstrated clearly that the endogenous lectin MBP, which is an important host defense component, binds endogenous ligand oligosaccharides expressed on the CD26 molecule on the surface of colon cancer cells with a characteristic high selectivity. This selectivity stems most probably from the geometric multiplicity of a blood group-type trisaccharide epitope, Le^b/Le^a, in the ligand oligosaccharides.

Material and methods

Materials

Chromatographic Media and Columns. CNBr-activated Sepharose 4B, protein G Sepharose 4B, and Sephadex G-10 were obtained from GE Healthcare UK Ltd (Buckinghamshire HP7 9NA, England). AAL-agarose was obtained from Seikagaku Biobusiness Corp. (Tokyo, Japan). MBP-agarose and monomeric avidin-agarose were obtained from Pierce-Thermo Fisher Scientific, Inc. (Rockford, IL). C18 Sep-Pak cartridge was obtained from Waters Corp. (Milford, MA).

Enzymes. PNGase F (peptide-N4-[acetyl-β-glucosaminyl] asparagines amidase) (*Flavobacterium meningosepticum*) was obtained from Boehringer Mannheim GmbH (Mannheim, Germany) or New England Bio Labs Inc. (Billerica, MA). Recombinant PNGase F (*N*-glycosidase F) from Roche Diagnostics GmbH (Mannheim, Germany). Endo-β-*N*-acetylglucosaminidase H (endo H) (*Streptomyces griseus*) was from Seikagaku Biobusiness Corp. Trypsin (mass spectrometry grade) was obtained from Promega Corp. (Madison, WI). α-Chymotrypsin (from bovine pancreas for biochemical use) was obtained from Wako Pure Chemical Industries (Tokyo, Japan).

Cells and Reagents for Cell Culture. SW1116 cells (ATCC CCL-233) were obtained from the American Type Culture Collection (Manassas, VA). Leibovitz's L-15 medium and trypsin-EDTA were from Invitrogen Corp. (Carlsbad, CA). Fetal calf serum (FCS) was from SAFC Biosciences (Lenexa, KS).

Antibodies. Anti-Le^b monoclonal IgG1 (clone 2-25 LE) was obtained from Seikagaku Biobusiness Corp. Mouse anti-human serum-MBP monoclonal IgG1 (clone HYB131-01) was obtained from BioPorto Diagnostics A/S (Gentofte, Denmark). Horseradish peroxidase-conjugated goat anti-mouse IgG (H+L) was obtained from Zymed-Invitrogen Corp. (Carlsbad, CA).

Other Reagents. Protease Inhibitor Cocktail for use with mammalian cell and tissue extracts was obtained from Nacalai Tesque, Inc. (Kyoto, Japan). Sulfo-NHS-biotin, colloidal Coomassie brilliant blue G-250 (GelCode Blue Stain Reagent), and Super Signal West Pico Chemiluminescent substrate were obtained from Pierce-Thermo Fisher Scientific, Inc. Horseradish peroxidase-conjugated streptavidin was obtained from Vector Laboratories, Inc. (Burlingame, CA). A nitrocellulose membrane was from Bio-Rad Laboratories, Inc. PVDF membrane and ULTRAFREE-10 K were from Millipore Corp. (Billerica, MA). A 5–20% polyacrylamide gradient gel (Tris-HCl) was from Atto Corp. (Tokyo, Japan). D-[1-^{3}H]glucosamine hydrochloride was obtained from American Radiolabeled Chemicals, Inc. (St. Louis, MO).

Chromatography buffers

PBS (−) was a 9.6 mM phosphate buffer, pH 7.5, containing 137 mM NaCl and 2.7 mM KCl. HBS was a 50 mM HEPES-NaOH buffer, pH 7.5, containing 150 mM NaCl. TBS was a 20 mM Tris-HCl buffer, pH 7.5, containing 150 mM NaCl. TBS# was a 20 mM Tris-HCl buffer, pH 7.5, containing 0.5 M NaCl. IBS was a 20 mM imidazole-HCl buffer, pH 7.8, containing 150 mM NaCl. HBS-N1 was HBS containing 1% Nonidet P-40. HBS-N2 was HBS containing 20 mM $CaCl_2$ and 0.1% Nonidet P-40. HBS-N3 was HBS containing 2 mM EDTA and 0.1% Nonidet P-40. HBS-N4 was HBS containing 0.1% Nonidet P-40. HBS-N5 was HBS containing 5 mM fucose, 2 mM EDTA, and 0.1% Nonidet-P40. IBS-N was IBS containing 0.1% Nonidet P-40. DEA-N was a 50 mM diethylamine-HCl buffer, pH 11.8, containing 0.1% Nonidet P-40. HBS-C1 was HBS containing 2 mM CHAPS and 20 mM $CaCl_2$. HBS-C2 was HBS containing 2 mM CHAPS and 2 mM EDTA. HBS-T1 was HBS containing 1% Triton X-100. HBS-T2 was HBS containing 1% Triton X-100, 5 mM fucose, and 2 mM EDTA. HBS-T3 was HBS containing 20 mM $CaCl_2$ and 1% Triton X-100. HBS-T4 was HBS containing 2 mM EDTA and 1% Triton X-100. TBS#-T1 was TBS# containing 1% Triton X-100. TBS#-T2 was TBS# containing 0.1% Triton X-100. DEA-T was a 50 mM diethylamine-HCl buffer, pH 11.5, containing 0.5 M NaCl and 0.1% Triton X-100. HBS-1 was HBS containing 20 mM $CaCl_2$. HBS-2 was HBS containing 2 mM EDTA. A 2% final concentration of the protease inhibitor mixture (Protease Inhibitor Cocktail for use with mammalian cell and tissue extract), comprising 100 mM PMSF, 80 mM aprotinin (bovine lung), 1.5 mM E-64, 2 mM leupeptin hemisulfate hydrate, 5 mM bestatin, and 1 mM pepstatin, was added to each buffer for the isolation of the cell surface MLGPs from the biotin-labeled cells and the MLGPs from cell lysates, and the purification of CD26 from cell lysates unless otherwise stated.

Cell culture and preparation of cell lysates from SW1116 cells

The culturing of a human colorectal carcinoma cell line, SW1116, and the preparation of cell lysates were carried out essentially according to the procedures described previously (Terada et al. 2005) except that to all buffers a protease inhibitor cocktail was added to a final concentration of 2%. The cell lysates were stored at −80°C until use.

Preparation of rabbit serum MBP and MBP-Sepharose 4B

Purification of MBP from normal rabbit serum on an affinity column of Sepharose 4B-mannan and coupling of the purified rabbit serum MBP to CNBr-activated Sepharose 4B were carried out according to the methods described previously (Terada et al. 2005). In this study, MBP-agarose (Pierce-Thermo Fisher Scientific, Inc.) was used as well as MBP-Sepharose 4B.

Preparation of an anti-Le^b monoclonal antibody (mAb)-Sepharose 4B

An anti-Le^b mAb (clone 2-25 LE, mouse IgG1) was coupled to CNBr-activated Sepharose 4B (2 mg protein per mL of gel) according to the manufacturer's instructions.

Preparations of anti-human CD26 mAb and anti-CD26 mAb-Sepharose 4B

Hybridoma cells producing an anti-human CD26 mAb (clone 44-4, mouse IgG1) were provided by the Department of Laboratory Medicine, Faculty of Medicine, University of Miyazaki. The anti-human CD26 mAb was purified from BALB/c mice ascites by ammonium sulfate precipitation, followed by chromatography on a protein G column. The purified anti-human CD26 mAb was coupled to CNBr-activated Sepharose 4B (3 mg protein per mL of gel).

Metabolic labeling of SW1116 cells with ^{3}H-glucosamine

In the pilot experiments for the monitoring of the glycopeptides prepared from the purified CD26, SW1116 cells were metabolically labeled with D-[1-^{3}H]glucosamine hydrochloride according to the procedure described previously (Terada et al. 2005). ^{3}H-labeled SW1116 cell lysates were prepared according to the procedures used for the preparation of the non-labeled cell lysates.

Cell surface labeling and preparation of surface-labeled cell lysates

SW1116 cells (1–3 × 10^7 cells/75 cm^2 flask) were washed twice with PBS (−) containing 2 mM EDTA and once with PBS (−), and then incubated in 1 mg/mL sulfo-NHS-biotin in PBS (−) at 4°C for 45 min with gentle shaking. The reaction was stopped by the addition of PBS (−) containing 20 mM glycine (pH 7.4) to the cells. After washing the cells with PBS (−), and then with HBS, the cells were lysed by gentle shaking for 30 min at 4°C in HBS-N1. Nuclei and insoluble substances were removed by centrifugation at 400 × *g* for 10 min, and then at 100,000 × *g* for 30 min at 4°C, respectively, and the supernatant was saved as the biotin-labeled cell lysates and kept at −80°C.

Isolation of MBP-ligand cell surface glycoproteins from the biotin-labeled SW1116 cells

To the cell lysates derived from SW1116 cells (11 flasks × 75 cm^2 flask), which had been surface-labeled with biotin, was added an equal volume of double concentration HBS-N2 (a calcium-containing buffer), followed by application to an MBP-affinity column (gel volume; 5 mL) equilibrated with HBS-N2. After the column had been washed with HBS-N2, the bound proteins were eluted with HBS-N3 (an EDTA-containing buffer). The fraction eluted from the MBP column was applied to a monomeric avidin column (gel volume; 5 mL) equilibrated with HBS-N4. The column was washed with HBS-N4, and then bound proteins were eluted with HBS-N4 containing 2 mM D-biotin. The bound fractions from the monomeric avidin column were resolved by SDS–PAGE on a 5–20% gradient gel, and then transferred to a nitrocellulose membrane. The membrane was treated with TBS containing 3% skim milk. After incubation of the membrane with horseradish peroxidase-conjugated streptavidin for 60 min at room temperature, the surface-biotinylated proteins were visualized with a chemiluminescent substrate kit according to the manufacturer's instructions.

Glycosidase digestion of biotinylated MBP-ligand glycoproteins

The MBP-binding glycoproteins were digested with 1.75 U of PNGase F (Boehringer Mannheim GmbH) or 5 mU of endo H at 37°C for 18 h in the presence of the protease inhibitor mixture. The samples before and after glycosidase digestions dissolved in HBS-N2 were applied to an MBP-affinity column, and the bound proteins were eluted with HBS-N3. The pass-through and bound fractions were resolved on a 5–20% polyacrylamide gradient gel and visualized with a chemiluminescent substrate kit.

Isolation and identification of glycoproteins carrying MBP-ligand oligosaccharides from SW1116 cell lysates

The cell lysates prepared from 2.5 flasks × 175 cm^2 flask (1 × 10^8 cells) were thawed, and then centrifuged at 10,000 × *g* for 20 min, and the supernatants were applied to an AAL column (gel volume; 0.5 mL), which had been equilibrated with HBS-N4. The column was washed with HBS-N4, and the bound glycoproteins were eluted with HBS-N5 (a fucose-containing buffer). The fraction bound on an AAL column was applied to an anti-Le^b mAb-Sepharose 4B column (gel volume; 0.5 mL), which had been equilibrated with IBS-N. The column was washed with IBS-N, and the bound glycoproteins were eluted with DEA-N (an alkaline buffer). The fractions eluted were immediately neutralized to pH 7.5, $CaCl_2$ was added to 20 mM, and then the fractions were applied to an MBP column (gel volume; 1 mL), which had been equilibrated with HBS-C1 (a calcium-containing buffer). The column was washed with HBS-C1, and the MBP-binding glycoproteins were eluted with HBS-C2 (an EDTA-containing buffer). The proteins eluted were concentrated by ultrafiltration (10 K membrane), and then resolved on a 5–20% polyacrylamide gradient gel and stained with colloidal Coomassie brilliant blue G-250. Bands were excised from the gel and subjected to *in-gel* digestion with trypsin. The peptides released from the gel were subjected to liquid chromatography/tandem mass spectrometry (LC-MS/MS) analysis using a hybrid quadrupole/time-of-flight mass spectrometer (Qstar Pulsar I; Applied Biosystems, Foster City, CA) interfaced on line with a capillary HPLC (Paradigm; Michrom BioResources, Inc., Auburn, CA) equipped with a Magic C18 column (0.2 × 50 mm, 3 μm; Michrom BioResources, Inc.). The eluents consisted of water containing 2% acetonitrile and 0.01% formic acid (pump A), and 90% acetonitrile and 0.01% formic acid (pump B), and the peptides were eluted with a linear gradient of 5–65% of pump B for 20 min at the flow rate of 2 mL/min. Data-dependent MS/MS acquisitions were performed on precursors with charge states of 2 or 3 over a survey mass range of 400–2000. Proteins were identified by searching the database of the National Center for Biotechnology Information using the ProID search engine (Applied Biosystems).

Glycosidase digestion of the MBP-ligand glycoproteins

The MBP-ligand glycoprotein fraction, which was eluted from an MBP-affinity column with HBS-C2, was concentrated by ultrafiltration as described above, and the concentrated MLGPs solution (3 μg/μL) was heated in a solution consisting of 0.1% SDS, 50 mM 2-mercaptoethanol, and 75 mM Tris-HCl buffer, pH 7.5, at 100°C for 5 min. An aliquot of the denatured proteins dissolved in 0.5% Nonidet P-40, 2 mM EDTA, 75 mM Tris-HCl, pH 7.5, and 0.03% PMSF was digested with 0.5 U of PNGase F (New England Bio Labs) at 37°C for 18 h. An aliquot of the denatured MBP-ligand protein solution was digested with 1.6 mU of endo H in a 100 mM citric acid-NaOH buffer, pH 5.5, and 0.03% PMSF at 37°C for 18 h.

MBP blotting of the MLGPs and their deglycosylated forms

Deglycosylated and control samples were resolved by SDS–PAGE on a 5–20% gradient gel, and then transferred to a PVDF membrane. After blocking the membrane with TBS containing 3% skim milk, the membrane was incubated first with 5.6 μg/mL MBP purified from human serum for 2–18 h, and then with mouse anti-human serum-MBP monoclonal IgG1 (10 μg/mL, HYB131-01) for 2 h, and finally with horseradish peroxidase-conjugated goat anti-mouse IgG (H+L) (1:1600 dilution) for 1 h. Each incubation was performed at room temperature in TBS containing 10 mM $CaCl_2$ and 3% skim milk, followed by three washes with TBS containing 10 mM $CaCl_2$ and 0.05% Tween 20. The protein bands were visualized with a chemiluminescent substrate kit as described above.

Purification of CD26 from SW1116 cell lysates

SW1116 cell lysates of 4.5 × 10^7 cells (28 flasks × 175 cm^2 flask), which had been kept at −80°C in TBS containing 1% Triton X-100 and 2% of protein inhibitor mixture, were thawed and

centrifuged at 11,000 × *g* for 20 min at 4°C, and the supernatant (140 mL) was applied to an AAL column (gel volume; 3 mL) equilibrated with HBS-T1. The column was washed with HBS-T1, and then the bound glycoproteins were eluted with HBS-T2 (a fucose-containing buffer). The fractions bound to an AAL column was pooled, diluted with five times volume of HBS-T3 (a calcium-containing buffer) to reduce a fucose concentration, and applied to an MBP column (gel volume; 3 mL). The MBP affinity chromatography was performed with HBS-T3 as the loading buffer and HBS-T4 (an EDTA-containing buffer) as the eluting buffer. The eluates were then applied to an anti-human CD26 mAb-Sepharose 4B column (gel volume: 0.7 mL) equilibrated with TBS#-T1. The column was washed with TBS#-T1, and then with TBS#-T2 to reduce a Triton X-100 concentration, and the proteins bound were eluted with DEA-T. The eluates were neutralized immediately, and then concentrated by ultrafiltration as described above. The concentrated CD 26 sample (approx. 25 μg protein, as estimated on densitography of the SDS–PAGE band) was mixed with 64 μL of SDS–PAGE sample buffer consisting of 12% SDS, 188 mM Tris-HCl buffer, pH 6.8, 15% 2-mercaptoethanol, and 30% glycerol, resolved on a 5–20% polyacrylamide gradient gel, and then stained with colloidal Coomassie brilliant blue G-250. The CD26 bands migrating to around 110 kDa were excised from the gel and subjected to *in-gel* digestion for further analyses.

Preparation of MBP-binding and non-MBP-binding fractions from chymotrypsin-digests of the CD26 purified from SW1116 cell lysates

CD26 was purified from cell lysates by means of an AAL column (gel volume: 4 mL), followed by an MBP-agarose column (gel volume: 5 mL), and then an anti-human CD26 mAb column (gel volume: 1 mL). The conditions for the AAL and MBP-affinity columns were the same as described above. The glycoproteins bound to an MBP column were applied to an anti-human CD26 mAb column equilibrated with TBS#-T1, and washed with TBS#-T2, and then with TBS#-T2 with no protease inhibitor mixture. The CD 26 bound to the column was eluted with DEA-T with no protease inhibitor mixture. The eluates were neutralized immediately with 2 M imidazole to pH 7.2. To remove Triton X-100 from the CD26 specimen (approx. 95 μg protein obtained from 70 flasks × 175 cm^2 flask (3×10^{10} cells)), trichloroacetic acid (TCA) was added to the purified CD26 solution to a final concentration of 10%, and the suspension was left standing on ice for 15 min, and then centrifuged at 20,000 × *g* for 15 min at 4°C. The precipitate was washed with 5% TCA, ethanol/0.2 M sodium acetate (8:2, v/v), and then 100% ethanol by centrifugation at 20,000 × *g* for 15 min at 4°C. The washed precipitate was dried up in a desiccator over silica gel, and then subjected to reduction and alkylation. The dried CD26 was dissolved in 7 M guanidine-HCl containing 0.5 M Tris-HCl, pH 8.5, and 2 mM EDTA, and then reduced by adding dithiothreitol to a final concentration of 2 mM, followed by incubation for 1 h at 50°C under nitrogen. The reduced CD26 was then carboxamidemethylated in the presence of iodoacetamide at a final concentration of 4 mM for 30 min at room temperature in the dark. To the CD26 solution, 2.5 volumes of methanol, 0.625 volumes of chloroform, and then 1.875 volumes of distilled water were added on ice with vigorous stirring, and the solution was centrifuged at 10,000 × *g* for 5 min at 4°C, and then the aqueous layer containing salts was removed. Then, to the CD26 protein present at the interface with the chloroform layer, 2.5 original sample volumes of methanol were added on ice, and after vigorous stirring, the mixture was centrifuged at 15,000 × *g* for 5 min at 4°C, and the precipitated CD26 was dried up and dissolved in the 0.1 M Tris-HCl buffer, pH 8.2, containing 6 M urea. Twenty microliters of the CD26 solution in 6 M urea was mixed with 80 μL of 0.1 M Tris-HCl buffer, pH 8.2 (final concentration of urea, 1.2 M), and denatured at 100°C for 10 min. After cooling down to room temperature, 1.9 μg of α-chymotrypsin (enzyme: substrate; 1:50 w/w) was added, and the solution was incubated at 37°C overnight. The digestion was stopped by heating at 100°C for 10 min, and the reaction mixture was subjected to centrifugation at 15,000 × *g* for 5 min at 4°C. The resulting supernatant was separated into MBP-binding and non-MBP-binding glycopeptides on an MBP-affinity column as follows. To the chymotrypsin digest of CD26 was added an equal volume of double concentration HBS-1 (a calcium-containing buffer), and then the solution was applied to an MBP-agarose column (gel volume: 1 mL) equilibrated with HBS-1, and the column was washed with HBS-1. The MBP-binding fraction was eluted with HBS-2 (an EDTA-containing buffer). The pass-through fraction (non-MBP-binding glycopeptides) and the eluted fraction (MBP-binding glycopeptides) were each subjected to gel filtration on a Sephadex G-10 column (column size: 1 × 14 cm) for desalting, and then the column was developed with a 10 mM ammonium bicarbonate buffer, pH 8.1. Each desalted glycopeptide fraction was pooled and subjected to further analyses.

MALDI-MS analysis of the N-glycans of CD26

The excised CD26 gel band was reduced with 50 mM dithioerythritol and alkylated with 65 mM iodoacetamide in the 100 mM ammonium bicarbonate buffer, pH 8.5, followed by destaining with 50% acetonitrile in the 50 mM ammonium bicarbonate buffer, pH 8.5. The *N*-linked glycans were then released by incubation overnight with PNGase F (Roche Diagnostics GmbH) in the 50 mM ammonium bicarbonate buffer, pH 8.5, and additionally extracted several times with water. The *N*-glycans from the isolated CD26 glycopeptide fractions (the MBP-binding and non-MBP-binding chymotryptic peptides separated on passing through an MBP column) were released directly with PNGase F in the 50 mM ammonium bicarbonate buffer, pH 8.5, and separated from de-*N*-glycosylated peptides by passing through a reverse-phase C18 Sep-Pak cartridge. All *N*-glycans collected from either source were permethylated using the NaOH/DMSO slurry method as described (Dell et al. 1994). For MALDI-TOF MS glycan profiling, the permethyl derivatives in acetonitrile were mixed 1:1 with a 2,5-dihydroxybenzoic acid (DHB) matrix (10 mg/mL in acetonitrile), spotted on the target plate, air-dried, and then recrystallized on-plate with acetonitrile. Data acquisition was performed on a 4700 Proteomics Analyzer (Applied Biosystems) operated in either the linear or reflectron mode.

Analysis of de-N-glycosylated peptides by MALDI and nanoLC-ESI-MS/MS

The MBP-binding and non-MBP-binding chymotryptic peptides were de-*N*-glycosylated with PNGase F (Roche Diagnostics GmbH), and then passed through a C18 Sep-pak cartridge to

remove the released *N*-glycans, as described above. The retained peptides were eluted with 25% and 50% acetonitrile containing 0.1% formic acid, the two eluates being combined for MS analysis. Automated nanoLC-ESI- MS/MS analysis was performed on a Micromass Q-Tof Ultima API mass spectrometer fitted with a nanoLC sprayer, a PepMap C18 m-precolumn cartridge (5 μm, 300 μm id × 5 mm; Dionex Corp., Sunnyvale, CA), and an analytical C18 capillary column (15 cm × 75 μm id, packed with 5 μm, Zorbax 300 SB C18 particles; Micro-Tech Scientific Inc., Vista, CA), at a flow rate of 300 nL/min using a 60 min gradient of 5–80% acetonitrile in 0.1% formic acid. Peptide identification was based on the searching of the MS/MS data against the CD26 sequence using the Mascot program with variable modifications set as N-terminal carbamylation, methionine oxidation, cysteine carboxyamidomethylation, and Asn to Asp conversion (deamidation), and not specifying the proteolytic enzyme. The raw MS/MS data for all peptide hits carrying the *N*-glycosylated sites were further examined and validated manually.

Modeling of tandem repeats of the Le^a unit

The structure information of Le^a trisaccharide was obtained from the literature (Yuriev et al. 2005). The dihedral angle of [GlcNAc C2]-[GlcNAc C1]-[O3Gal]-[C3Gal] was assumed to be 180° taking into account the exo anomeric effect (Rao et al. 1998). Among the three possible dihedral angles (180°, −60°, and 60°) for [GlcNAc C1]-[O3Gal]-[C3Gal]-[C2 Gal], the angle of 180° generated a stable helical structure. The resulting eight tandem repeats of the Le^a unit were then covered by water molecules of 5.0 Å thick in VEGA OpenGL v.1.5.1, (Pedretti et al. 2002) and energy-minimized with molecular mechanics calculation using MMFF94 force field in Spartan06 (Wavefunction, Inc., Irvine, CA).

Modeling of MLO-non-reducing terminal oligosaccharide structures

Oligosaccharide structures were constructed by use of the carbohydrate module installed in InsightII (Molecular Simulations Inc., San Diego, CA) and the structures were energy-minimized using Discover3 until rmsd becomes less than 0.01 kcal/mol. Molecular dynamics calculations for structure-optimization were performed at 300 K for 100 ps using Discover3. The initial conformation of the Le^a unit constructed by connecting galactose, GlcNAc, and fucose was energy-minimized by molecular mechanics and optimized by molecular dynamics calculation. The optimized conformation of Le^a was very close to the conformation observed in the complex structure bound in the protein (pdb code: 1 W8H). Thus, the Le^a unit was used for further construction of the oligomeric tandem structure. The dimeric structure with the GlcNAc(β1-3)Gal moiety was generated at the glycosidic bond with anti-conformations (dihedral angles of 180°), and then the structure was energy-minimized. The conformational search at the glycosidic bonds using the program EMBRACE installed in the molecular modeling program Maestro (Schrödinger Inc., Portland, OR) resulted in the preferred conformation of the glycosidic bond, which was close to the initial structure. Thus, the other glycosidic bonds were also constructed at the dihedral angles of 180°. To complete the MLO-terminal oligosaccharide, Le^b–(Le^a)$_4$–Le^x, fucose was then attached to the Gal at the non-reducing terminal end with an α1-2 glycosidic bond. At the reducing terminal, the Le^x moiety was attached through a β1-3 glycosidic bond. The resulting whole oligosaccharide fragment was then covered by water molecules of 10 Å thickness and energy-minimized by molecular mechanics.

Modeling of the MBP-Lewis oligosaccharide complex

The crystal structure of the trimeric mannan (mannose)-binding protein (pdb code: 1 kww) was used for building the complex model with the oligosaccharide fragment. Regarding the binding mode of mannose in the crystal structure of the mannan (mannose)-binding protein (pdb code: 2 msb), the fucose moiety was placed at the mannose-binding site of the protein by binding the *trans*-diequatorial hydroxyl groups with the calcium atom bound at the binding site. Of the two fucose residues at the non-reducing terminal, the fucose attached to the terminal Le^a moiety well fit without severe steric interactions with the protein moiety. Moreover, each oligosacharide bound to the trimeric structure was found to be located so as to form a bundle at the Le^x portion. On the other hand, the binding of the other fucose in the terminal Le^a moiety showed steric interactions with the protein, which was not successfully removed by rotating a few glycosidic bonds. The complex structure was then covered by water molecules of 10 Å thickness and energy-minimized by molecular mechanics.

Funding

A grant-in-Aid for Scientific Research on Priority Areas [14082203 to T.K.] from the Ministry of Education, Culture, Sports, Science and Technology of Japan; grant-in-aids for Scientific Research [C-16590046 and C-18590053 to N.K., B-18370057 to T.K.], Core-to-Core Program-Strategic Research Networks [17005] from the Japan Society for the Promotion of Sciences of Japan; and a Taiwan National Science Council grant [95-3112-B-001-014 to K-H. K.].

Acknowledgements

The authors would like to thank Dr. Kathleen Aertgeerts and Cold Spring Harbor Laboratory Press for permission to reproduce Figure 1B of the article "*N*-linked glycosylation of dipeptidyl peptidase IV (CD26): Effects on enzyme activity, homodimer formation, and adenosine deaminase binding" (Aertgeerts et al. 2004) as Figure 7 in this article. The authors are grateful to Drs. Tomio Kotani, Yatsuki Aratake, and Kazumi Umeki at the Department of Laboratory Medicine, Faculty of Medicine, University of Miyazaki, for their kind cooperation in preparation of anti-human CD26 mAb for us, and Ms. Tomoko Tominaga for the secretarial assistance. Mass spectrometry analyses of the glycans and glycopeptides were performed at the NRPGM Core Facilities for Proteomics located at the Institute of Biological Chemistry, Academia Sinica. Protein ID by LC-MS/MS was performed at the Division of Biological Chemistry and Biologicals, National Institute of Health Science. 3D modeling of tandem repeats of the Le^a unit was carried out in the Faculty of Applied Biological Science, Gifu University, and modeling of the MBP-Lewis oligosaccharides complex was performed in the Suntory Institute for Bioorganic Research.

Conflict of interest statement

None declared.

Abbreviations

AAL, *Aleuria aurantia* lectin; CD98hc, CD98 heavy chain; CHAPS, 3-[(3-Cholamidopropyl)dimethyl-ammonio]-1-propane sulfonate; CRD, carbohydrate-recognition domain; DPPIV, dipeptidyl peptidase IV; endo H, endo-β-*N*-acetylglucosaminidase H; Hex, hexose; HexNAc, *N*-acetylhexosamine; LacCer, lactosylceramide; LacNAc, *N*-acetyllactosamine; LC-MS/MS, liquid chromatography/tandem mass spectrometry; Le^a, Lewis a; Le^b, Lewis b; Le^x, Lewis x; mAb, monoclonal antibody; MALDI, matrix-assisted laser desorption/ionization; MBP, mannan-binding protein; MDCC, MBP-dependent cell-mediated cytotoxicity; MLGP, MBP-ligand glycoprotein; MLO, MBP-ligand oligosaccharides; MS, mass spectrometry; nanoLC-ESI-MS/MS, nano liquid chromatography/electrospray ionization/tandem mass spectrometry; TOF, time-of-flight.
All of the sugar residues have the D-configuration except fucose, which has the L-configuration.

References

Aertgeerts K, Ye S, Shi L, Prasad SG, Witmer D, Chi E, Sang B-C, Wijnands RA, Webb DR, Swanson RV. 2004. *N*-Linked glycosylation of dipeptidyl peptidase IV (CD26): Effects on enzyme activity, homodimer formation, and adenosine deaminase binding. *Protein Sci*. 13(1):145–154.

Asano S, Kameyama M, Oura A, Morisato A, Sakai H, Tabuchi Y, Chairoungdua A, Endou H, Kanai Y. 2007. L-Type amino acid transporter-1 expressed in human astrocytomas, U343MGa. *Biol Pharm Bull*. 30(3):415–422.

Dell A, Reason AJ, Khoo K-H, Panico M, McDowell RA, Morris HR. 1994. Mass spectrometry of carbohydrate-containing biopolymers. *Methods Enzymol*. 230:108–132.

Dommett RM, Klein N, Turner MW. 2006. Mannose-binding lectin in innate immunity: Past, present and future. *Tissue Antigens*. 68(3):193–209.

Esseghir S, Reis-Filho JS, Kennedy A, James M, O'Hare MJ, Jeffery R, Poulsom R, Isacke CM. 2006. Identification of transmembrane proteins as potential prognostic markers and therapeutic targets in breast cancer by a screen for signal sequence encoding transcripts. *J Pathol*. 210(4):420–430.

Fan Y-Y, Yu S-Y, Ito H, Kameyama A, Sato T, Lin C-H, Yu L-C, Narimatsu H, Khoo K-H. 2008. Identification of further elongation and branching of dimeric type 1 chain on lactosylceramides from colonic adenocarcinoma by tandem mass spectrometry sequencing analyses. *J Biol Chem.* 283(24):16455–16468.

Hara K, Kudo H, Enomoto T, Hashimoto Y, Masuko T. 2000. Enhanced tumorigenicity caused by truncation of the extracellular domain of GP125/CD98 heavy chain. *Oncogene.* 19(54):6209–6215.

Havre PA, Abe M, Urasaki Y, Ohnuma K, Morimoto C, Dang NH. 2008. The role of CD26/dipeptidyl peptidase IV in cancer. *Front Biosci.* 13(5):1634–1645.

Hoffmann JA, Kafatos FC, Janeway CA, Ezekowitz RA. 1999. Phylogenetic perspectives in innate immunity. *Science.* 284(5418):1313–1318.

Huang J, Byrd JC, Yoon WH, Kim YS. 1992. Effect of benzyl-alpha-GalNAc, an inhibitor of mucin glycosylation, on cancer-associated antigens in human colon cancer cells. *Oncol Res.* 4(11-12):507–515.

Ikeda K, Sannoh T, Kawasaki N, Kawasaki T, Yamashina I. 1987. Serum lectin with known structure activates complement through the classical pathway. *J Biol Chem.* 262(16):7451–7454.

Inamoto T, Yamada T, Ohnuma K, Kina S, Takahashi N, Yamochi T, Inamoto S, Katsuoka Y, Hosono O, Tanaka H, et al. 2007. Humanized anti-CD26 monoclonal antibody as a treatment for malignant mesothelioma tumors. *Clin Cancer Res.* 13(14):4191–4200.

Inamoto T, Yamochi T, Ohnuma K, Iwata S, Kina S, Inamoto S, Tachibana M, Katsuoka Y, Dang NH, Morimoto C. 2006. Anti-CD26 monoclonal antibody-mediated G1-S arrest of human renal clear cell carcinoma Caki-2 is associated with retinoblastoma substrate dephosphorylation, cyclin-dependent kinase 2 reduction, $p27^{kip1}$ enhancement, and disruption of binding to the extracellular matrix. *Clin Cancer Res.* 12(11):3470–3477.

Iwata S, Morimoto C. 1999. CD26/dipeptidyl peptidase IV in context. The different roles of a multifunctional ectoenzyme in malignant transformation. *J Exp Med.* 190(3):301–305.

Kawasaki N, Kawasaki T, Yamashina I. 1983. Isolation and characterization of a mannan-binding protein from human serum. *J Biochem.* 94(3):937–947.

Kawasaki N, Kawasaki T, Yamashina I. 1989. A serum lectin (mannan-binding protein) has complement-dependent bactericidal activity. *J Biochem.* 106(3):483–489.

Kawasaki T. 1999. Structure and biology of mannan-binding protein, MBP, an important component of innate immunity. *Biochim Biophys Acta*. 1473(1):186–195.

Ma Y, Uemura K, Oka S, Kozutsumi Y, Kawasaki N, Kawasaki T. 1999. Antitumor activity of mannan-binding protein in vivo as revealed by a virus expression system: Mannan-binding protein dependent cell-mediated cytotoxicity. *Proc Natl Acad Sci USA*. 96(2):371–375.

Malhotra R, Lu J, Holmskov U, Sim RB. 1994. Collectins, collectin receptors and the lectin pathway of complement activation. *Clin Exp Immunol.* 97(Suppl. 2):4–9.

Muto S, Sakuma K, Taniguchi A, Matsumoto K. 1999. Human mannose-binding lectin preferentially binds to human colon adenocarcinoma cell lines expressing high amount of Lewis A and Lewis B antigens. *Biol Pharm Bull.* 22(4):347–352.

Ohnuma K, Ishii T, Iwata S, Hosono O, Kawasaki H, Uchiyama M, Tanaka H, Yamochi T, Dang NH, Morimoto C. 2002. G1/S cell cycle arrest provoked in human T cells by antibody to CD26. *Immunology.* 107(3):325–333.

Ohta M, Kawasaki T. 1994. Complement-dependent cytotoxic activity of serum mannan-binding protein towards mammalian cells with surface-exposed high-mannose type glycans. *Glycoconj J.* 11(4):304–308.

Pedretti A, Villa L, Vistoli G. 2002. VEGA: A versatile program to convert, handle and visualize molecular structure on Windows-based PCs. *J Mol Graph Model*. 21(1):47–49.

Pro B, Dang NH. 2004. CD26/dipeptidyl peptidase IV and its role in cancer. *Histol Histpathol.* 19(4):1345–1351.

Rao VSR, Qasba PK, Balaji PV, Chandrasekaran R. 1998. Conformation of Carbohydrates. Amsterdam: Harwood Academic Publishers.

Super M, Thiel S, Lu J, Levinsky RJ, Turner MW. 1989. Association of low levels of mannan-binding protein with a common defect of opsonisation. *Lancet.* 2(8674):1236–1239.

Takahashi K, Ip WE, Michelow IC, Ezekowitz RA. 2005. The mannose-binding lectin: A prototypic pattern recognition molecule. *Curr Opin Immunol.* 18(1):16–23.

Taylor ME, Drickamer K. 2007. Paradigms for glycan-binding receptors in cell adhesion. *Curr Opin Cell Biol.* 19(5):572–577.

Terada M, Khoo K-H, Inoue R, Chen C-I, Yamada K, Sakaguchi H, Kadowaki N, Ma BY, Oka S, Kawasaki T, et al. 2005. Characterization of oligosaccharide ligands expressed on SW1116 cells recognized by mannan-binding protein. A highly fucosylated polylactosamine type *N*-glycan. *J Biol Chem.* 280(12):10897–10913.

Yamashita K, Kochibe N, Ohkura T, Ueda I, Kobata A. 1985. Fractionation of L-fucose-containing oligosaccharides on immobilized *Aleuria aurantia* lectin. *J Biol Chem.* 260(8):4688–4693.

Yuriev E, Farrugia W, Scott AM, Ramsland PA. 2005. Three-dimensional structures of carbohydrate determinants of Lewis system antigens: Implications for effective antibody targeting of cancer. *Immunol Cell Biol.* 83(6):709–717.